ELSEVIER

Nuclear Medicine and Biology 28 (2001) 959–973

NUCLEAR MEDICINE — AND — BIOLOGY

Stereoselective synthesis, *in vitro*, and initial *in vivo* evaluation of 1-methylpiperidin-4-yl α-hydroxy-α-(1-iodo-1-propen-3-yl)-α-phenylacetate (IPIP): a novel radioiodinated molecular probe with high affinity for the muscarinic receptor

Daniel W. McPherson*, William K. Breeden, Arnold L. Beets, Huimin Luo, Victor Sood, Furn F. Knapp Jr.

Nuclear Medicine Group, Life Sciences Division, Oak Ridge National Laboratory (ORNL), Post Office Box 2008, Building 4501, Oak Ridge, TN 37831-6229, USA

Received 5 May 2001; received in revised form 5 June 2001; accepted 9 June 2001

Abstract

1-Methylpiperidin-4-yl α-hydroxy-α-(1-iodo-1-propen-3-yl)-α-phenylacetate (IPIP, Fig. 1) was investigated as a potential radioiodinated molecular probe targeted to the muscarinic receptor complex. The IPIP stereoisomers were synthesized *via* a chiral intermediate in >95% enantiomeric excess. The R-isomers demonstrated a M_1 to M_2 subtype selectivity of approximately 3 to 1 and the S-isomers demonstrated non-subtype selective binding *in vitro*. IPIP was radiolabeled with iodide-125 with an average radiochemical yield of 74.4% ($\pm$14.8, n = 5), specific activities >800 mCi/μmol, and radiochemical purities >97%. *In vivo* the Z-isomers demonstrated high uniform cerebral uptake suggesting non-subtype selective binding. In contrast, E-R-IPIP, after allowing a low uptake in M_2 rich areas to clear, demonstrated a retention of activity in M_1 and M_4 rich cerebral regions. In addition, the cerebral uptake of E-R-IPIP and Z-S-IPIP were inhibited by 70–90% *via* pretreatment with R-QNB, an established muscarinic antagonist. An *ex vivo* metabolism study demonstrated Z-S-IPIP was stable at the receptor site with an absence of radiolabeled metabolites. © 2001 Elsevier Science Inc. All rights reserved.

Keywords: IPIP; Muscarinic; Receptor; Iodine-125; Stereoisomers

1. Introduction

The muscarinic acetylcholinergic receptor (mAChR) complex consists of five subtypes (M_1-M_5) as determined by molecular cloning techniques and are located throughout the brain in varying concentrations [9,19,21]. *It has been recently suggested a common designation for the five muscarinic receptor subtypes be denoted by M_1–M_5 to reflect their order of discovery* [13]. The individual mAChR subtypes are postulated to play important roles in the normal aging process in addition to memory dysfunction, schizophrenia, Parkinson's, and Alzheimer's disease [3,11,14,15, 20,31,33,50].

These observations have spurred interest in the development of radiolabeled molecular probes for the non-invasive imaging of mAChR by nuclear medicine techniques. The development of an appropriate radiolabeled molecular probe targeted to an individual mAChR subtype has the potential to afford a window into the biological role of mAChR in healthy and diseased tissues. In addition, a subtype selective molecular probe has potential for a cost-effective differential diagnosis for various dementias and to aid in the monitoring of new and existing drug modalities for the treatment of various diseases.

Iodine-123-labeled R-3-quinuclidinyl S-4-iodophenylbenzilate (IQNB, Fig. 1), an analogue of R-3-quinuclidinyl benzilate (R-QNB, Fig. 1), and iododexetimide (IDEX, Fig. 1) have been utilized for the clinical non-invasive *in vivo* imaging of mAChR density *via* single photon emission computed tomography (SPECT) [6,7,10,12,17,27,28,41,42, 44–48]. However, these molecular probes are not subtype selective and exhibit relatively slow dissociation rates from the binding sites limiting the estimation of binding site density *in vivo* [6,42].

* Corresponding author. Tel.: +1-301-435-1175; fax: +1-301-480-2241.

E-mail address: mcphersod@CSR.NIH.GOV (D.W. McPherson).

0969-8051/01/$ – see front matter © 2001 Elsevier Science Inc. All rights reserved.
PII: S0969-8051(01)00252-9

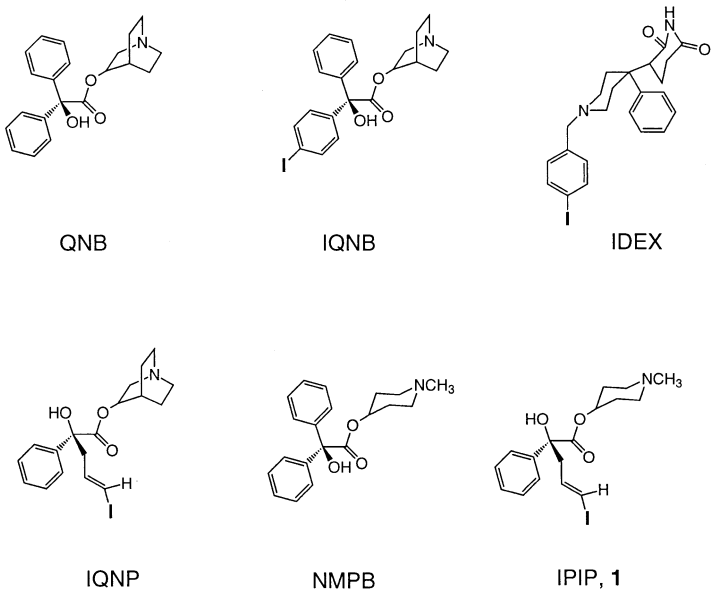

Fig. 1. QNB and various radiolabeled mAChR antagonists.

To overcome the limitations of these molecular probes, we had developed a novel QNB analogue, 1-azabicyclo[2.2.2]oct-3-yl α-hydroxy-α-(1-iodo-1-propen-3-yl)-α-phenylacetate (IQNP, Fig. 1) with respect to cerebral uptake, subtype selectivity, and *in vivo* receptor binding [4,5,22,23,26,29,30,32]. E-RR-IQNP demonstrated an 80 fold selectivity for the M_1, M_4 subtype *in vitro* and significant binding to cerebral regions containing a high concentration of the M_1, M_4 subtype after allowing time for clearance of the measurable M_2 subtype binding *in vivo.* In addition, Z-RR-IQNP, although non-subtype selective *in vitro* and *in vivo,* for the first time demonstrated significant receptor binding to cerebral regions containing a high M_2 subtype concentration.

However, initial SPECT imaging studies utilizing healthy volunteers demonstrated a wide range of inter-individual values for both time of peak equilibration and binding potential values limiting the utility of this new molecular probe [29]. Although E-RR-IQNP demonstrates attractive mAChR subtype binding profile and cerebral uptake, the slow pharmacokinetics in the human brain is a major disadvantage that must be overcome to be useful as mAChR specific molecular probes in routine clinical diagnostic studies. The reported slow release from the receptor pocket of various 3-quinuclidinyl esters has been postulated to directly relate to a high nanomolar binding affinity of these molecular probes. Therefore to obtain a more favorable *in vivo* ligand-receptor-binding interaction a decrease in the binding affinity is desired.

It has been reported the binding affinity of the ligand can be influenced *via* modification of the nitrogen containing heterocycle moiety [36,43]. Carbon-11-labeled N-methylpiperidin-4-yl benzilate (NMPB, Fig. 1), in which the 3-quinuclidinyl moiety of QNB was modified to a 1-methylpiperidin-4-yl moiety, was investigated as a potential ligand for the evaluation of mAChR density *via* Positron Emission Tomography (PET) [1,2,35,38–40,49,51]. Although this modification to the QNB structure afforded a molecular probe with the desired decrease in binding affinity, NMPB does not discriminate between mAChR subtypes.

We now report the stereoselective synthesis, radioiodination, *in vitro* and initial *in vivo* evaluation of 1-methylpiperidin-4-yl α-hydroxy-α-(1-iodo-1-propen-3-yl)-α-phenylacetate (IPIP, Fig. 1), a novel IQNP analogue in which the 3-quinuclidinyl ester moiety has been replaced by the 1-methylpiperidin-4-yl moiety. We have previously reported a dosimetric study for Z-S-IPIP [8].

2. Materials and methods

2.1. General

Tributyltin hydride, carbonyldiimidazole (CDI), anhydrous DMF, anhydrous THF, and 4-hydroxy-1-methylpiperidine were purchased from Aldrich Chemical Company (Milwaukee, WI). All other reagents were of analytical grade and used without further purification. R and S-ethyl α-hydroxy-α-phenyl-α-(1-propyn-3-yl)acetate (**5**), R and S α-hydroxy-α-phenyl-α-(1-propyn-3-yl)acetic acid (**2**) and R-QNB were prepared as previously reported [24,34]. Sodium iodine-125 (specific activity 17 Ci/mg) was obtained from New England Nuclear Life Sciences Division (Roxbury, MA). Human cloned M_1 and M_2 receptors were purchased from Receptor Biology, Inc (Beltsville, MD). [N-Methyl-^{3}H]-scopolamine methyl chloride (specific activity 82 Ci/mmol) was obtained from NEN Life Sciences Products, Inc. (Boston, MA). C-18 Sep Pak cartridges were

purchased from Waters Corporation (Cary, NC). Proton (^{1}H) and carbon (^{13}C) NMR was obtained utilizing a Varian Gemini 200 instrument (Palo Alto, CA). Proton spectra are reported using tetramethylsilane (0.00 ppm) and carbon spectra are reported using chloroform (77.0 ppm) as reference standards. Melting points were determined using a Hoover melting point Model 245 apparatus and are reported uncorrected. Optical rotation was obtained utilizing a Perkin-Elmer Model 341 polarimeter. Analytical high performance liquid chromatography (HPLC) was performed with an isocratic Waters system consisting of a Model 515 pump and Model 996 Photodiode detector with Millenium[32] Chromatography Manager (Cary, NC). A mobile phase of CH_2Cl_2/[CH_3CH_2OH + 1% $N(CH_2CH_3)_3$] [98:2 for IPIP (**1**), 99:1 for TBTPIP (**4**)], flow rate of 1.0 mL/min and a Waters μPorasil column (1.7 mm × 30 cm) were utilized. Semi-preparative HPLC was performed with a Waters Model 510 HPLC pump and Model 454 variable UV detector (254 nm) (Cary, NC) utilizing a Beckman Model 170 radioisotope flow detector (Fullerton, CA). The HPLC conditions for the purification of the radioiodinated IPIP stereoisomers utilized a mobile phase of CH_2Cl_2/[CH_3CH_2OH + 1% $N(CH_2CH_3)_3$] [98:2], flow rate of 2.5 mL/min and a Waters semi-preparative μPorasil column (3.9 mm × 30 cm). Radiochemical thin layer chromatographic (RTLC) analysis was performed using Analtech glass coated silica GF plates (250 micron) (Newark, DE.) and a mobile phase of $CHCl_3$/CH_3OH (8.5:1.5). The plates were analyzed using a Bioscan System 200 Imaging Scanner with an Autochanger 1000 (Washington, DC). Elemental analyses were obtained from Galbraith Laboratories, Inc. (Knoxville, TN).

2.2. Synthesis

2.2.1. (R)-1-Methylpiperidin-4-yl α-hydroxy-α-phenyl-α-(1-propyn-3-yl)acetate (R-3)

2.2.1.1. Activated ester approach. A solution of **R-2** (1.69 g, 8.9 mmol) and carbonyldiimidazole (CDI) (1.58 g, 9.7 mmol) in anhydrous DMF (30 mL) was stirred at room temperature under positive argon pressure for 2 h. A solution of 4-hydroxy-1-methylpiperidine (2.59 g, 22.5 mmol) in anhydrous DMF (10 mL) was added and the resultant solution was stirred at 80°C under positive argon pressure for 18 h. The solution was cooled to room temperature, diluted with ice water (200 mL), and washed twice with ethyl acetate (200, 100 mL). The organic washes were combined, dried over anhydrous $MgSO_4$, and evaporated to dryness to afford an orange oil. Purification by flash column chromatography [silica, $CHCl_3$/CH_3OH/NH_4OH (94:5:1)] afforded **R-3** as an orange oil (1.18 g, 46.1%). TLC [silica, $CHCl_3$/CH_3OH (9:1)] R_f = 0.54. ^{1}H NMR δ 7.63–7.57 (m, 2H), 7.40–7.29 (m, 3H), 4.95–4.88 (m, 1H), 4.10 (m, 1H), 3.22–3.13 (dd, 1H), 2.88–2.78 (dd, 1H), 2.62–1.60 (m, 8H), 2.25 (s, 3H), 2.04 (t, 1H). ^{13}C NMR δ 172.7, 140.0, 128.1, 128.0, 125.3, 79.1, 77.2, 72.0, 70.9, 52.2, 46.1, 30.9, 30.1, 30.2. $[\alpha]^D = -22.47°$ ($CHCl_3$, c = 29.2 mg/mL).

2.2.1.2. Transesterification approach. A solution of 1-methyl-4-hydroxypiperidine (1.90 g, 16.5 mmol) in benzene (50 mL) was refluxed utilizing a Dean-Stark trap for 1 h under positive argon pressure. The solution was cooled to room temperature and the benzene collected in the trap was discarded. Freshly cut sodium metal (0.5 g, 21.7 mmol) was added and the solution refluxed under positive argon pressure utilizing a Dean Stark trap for 1 h. The solution was cooled slightly and transferred warm under positive argon pressure to a solution of R-(-)-ethyl α-hydroxy-α-phenyl-α-(1-propyn-3-yl)acetate (**5**) (994.6 mg, 4.6 mmol) in 50 mL of anhydrous benzene. The resultant solution was refluxed under positive argon pressure utilizing a Dean Stark trap for 18 h. The solution was then cooled to room temperature, poured into water (200 mL) and washed with ethyl acetate (2 × 150 mL). The organic fractions were combined, washed with water (100 mL), dried over anhydrous $MgSO_4$, and evaporated to dryness to afford an orange oil. The product was purified by flash column chromatography ($CHCl_3$/CH_3OH/NH_4OH [94:5:1]) to afford a single spot *via* TLC (silica, $CHCl_3$/CH_3OH [9:1] R_f = 0.54) containing a mixture of **R-3** and (R)-1-methylpiperidin-4-yl α-(allenyl)-α-hydroxy-α-phenylacetate (**6**) in approximately 1 to 1 molar ratio (499.8 mg, 37.8%).

2.2.2. Compound 6 ^{1}H NMR (from the mixture)

δ 7.62–7.56 (m, 2H), 7.40–7.24 (m, 3H), 5.75 (t, 1H), 4.99–4.95 (d, 2H), 4.95–4.88 (m, 1H), 4.10 (m, 1H), 2.62–1.60 (m, 8H), 2.25 (s, 3H). ^{13}C NMR δ 172.7, 140.8, 140.0, 128.1, 127.9, 125.3, 95.3, 79.1, 77.2, 71.9, 71.0, 52.0, 46.1, 30.9, 30.1, 30.2.

2.2.3. (S)-1-Methylpiperidin-4-yl α-hydroxy-α-phenyl-α-(1-propyn-3-yl)acetate (S-3)

Utilizing the activated ester approach, **S-3** was prepared with **S-2** (1.87 g, 9.8 mmol), CDI (1.60 g, 9.9 mmol), and 4-hydroxy-1-methylpiperidine (4.63 g, 40.2 mmol) to afford **S-3** as an orange oil (1.15 g, 40.9%). TLC [silica, $CHCl_3$/CH_3OH (9:1)] R_f = 0.54. ^{1}H NMR δ 7.62–7.56 (m, 2H), 7.39–7.27 (m, 3H), 4.94–4.87 (m, 1H), 3.21–3.11 (dd, 1H), 2.90–2.84 (dd, 1H), 2.79–2.14 (m, 4H), 2.22 (s, 3H), 2.04 (t, 1H), 2.03–1.67 (m, 4H). ^{13}C NMR δ 172.6, 140.3, 128.1, 128.0, 125.3, 79.3, 77.2, 71.8, 71.0, 52.2, 46.1, 31.0, 30.2, 30.1. $[\alpha]^D = +22.36°$ ($CHCl_3$, c = 28.7 mg/mL).

2.2.4. E-(S)-1-Methylpiperidin-4-yl α-hydroxy-α-phenyl-α-(1-tributylstannyl-1-propen-3-yl)acetate (E-S-4)

A solution of **S-3** (513.9 mg, 1.8 mmol), AIBN (367.7 mg, 2.3 mmol) and tributyltin hydride (757.4 mg, 2.6 mmol) in anhydrous toluene (10 mL) was stirred under positive argon pressure at 75°C for 18 h. The solution was cooled to room temperature, diluted with CH_2Cl_2 (200 mL) and washed with water (100 mL). The organic solution was dried over anhydrous $MgSO_4$ and evaporated to dryness. The product was purified by flash column chromatography [silica, $CHCl_3$/CH_3OH/NH_4OH (96:3:1)] to afford **E-S-4** as

a pale oil (713.2 mg, 52.8%). TLC [silica, $CHCl_3/CH_3OH$ (9:1)] R_f = 0.65. ^1H NMR δ 7.64–7.59 (m, 2H), 7.38–7.26 (m, 3H), 6.16–6.06 (d, 1H, J = 18.9 Hz), 5.99–5.96 (t, 1H), 4.84–4.79 (m, 1H), 3.88 (s, 1H), 3.11–3.01 (dd, 1H), 2.86–2.77 (dd, 1H), 2.58–2.17 (m, 4H), 2.25 (s, 3H), 1.92–1.61 (m, 4H), 1.54–1.38 (m, 6H), 1.33–1.19 (m, 6H), 0.91–0.80 (m, 15H). ^{13}C NMR δ 174.0, 142.2, 141.5, 133.9, 128.0, 127.5, 125.5, 77.9, 71.7, 52.5, 48.2, 46.2, 30.7, 30.4, 29.1, 27.3, 13.7, 9.5. HPLC analysis: retention time = 9.0 min. $[\alpha]^D$ = +20.46° ($CHCl_3$, c = 65.0 mg/mL).

*2.2.5. E-(R)-1-Methylpiperidin-4-yl α-hydroxy-α-phenyl-α-(1-tributylstannyl-1-propen-3-yl)acetate (***E-R-4***)*

E-R-4 was prepared as above with **R-3** (469.3 mg, 1.6 mmol), AIBN (317.2 mg, 1.9 mmol) and tributyltin hydride (649.2 mg, 2.2 mmol) to afford **E-R-4** as a pale oil (595.0 mg, 64.3%). TLC [silica, $CHCl_3$/CH3OH (9:1)] R_f = 0.68. ^1H NMR δ 7.64–7.59 (m, 2H), 7.38–7.26 (m, 3H), 6.16–6.06 (d, 1H, J = 19.0 Hz), 6.02–5.96 (t, 1H), 4.87–4.79 (m, 1H), 3.85 (s, 1H), 3.13–3.01 (dd, 1H), 2.87–2.77 (dd, 1H), 2.63–2.10 (m, 4H), 2.26 (s, 3H), 2.00–1.22 (m, 16H), 1.65–1.10 (m, 15H). ^{13}C NMR δ 174.0, 142.2, 141.49, 134.0, 128.0, 127.5, 125.5, 77.9, 71.7, 52.5, 48.2, 46.2, 30.7, 30.4, 29.1, 27.3, 13.8, 9.5. HPLC analysis: retention time = 9.6 min. $[\alpha]^D$ = −20.56° ($CHCl_3$, c = 46.7 mg/mL).

*2.2.6. Z-(S)-1-Methylpiperidin-4-yl α-hydroxy-α-phenyl-α-(1-tributylstannyl-1-propen-3-yl)acetate (***Z-S-4***)*

A solution of **S-3** (845.6 mg, 2.9 mmol) and tributyltin hydride (3.25 g, 11.2 mmol) in anhydrous HMPA (6 mL) was stirred under positive argon pressure at 75°C for 5 d. The solution was cooled to room temperature and the HMPA was removed by Kugelrohr distillation at 70°C under high vacuum. The product was purified by repeated flash column chromatography [silica, $CHCl_3/CH_3OH/NH_4OH$ (96:3:1)] to afford **Z-S-4** as a pale oil (239.6 mg, 14.3%). TLC [silica, $CHCl_3/CH_3OH$ (9:1)] R_f = 0.60. ^1H NMR δ 7.64–7.57 (m, 2H), 7.39–7.24 (m, 3H), 6.49–6.36 (pent, 1H), 6.07–6.00 (d, 1H, J = 12.7 Hz), 4.91–4.84 (m, 1H), 3.70 (bs, 1H), 3.03–2.91 (dd, 1H), 2.82–2.70 (dd, 1H), 2.68–2.19 (m, 4H), 2.25 (s, 3H), 2.11–1.64 (m, 4H), 1.57–1.41 (m, 6H), 1.38–1.20 (m, 6H), 0.96–0.84 (m, 15H). ^{13}C NMR δ 174.0, 141.6, 141.3, 133.7, 128.1, 127.6, 125.5, 77.5, 71.9, 52.4, 52.4, 46.3, 30.7, 30.4, 29.2, 27.4, 13.8, 10.3. HPLC analysis: retention time = 11.5 min. $[\alpha]^D$ = +19.20° ($CHCl_3$, c = 45.2 mg/mL).

*2.2.7. Z-(R)-1-Methylpiperidin-4-yl α-hydroxy-α-phenyl-α-(1-tributylstannyl-1-propen-3-yl)acetate (***Z-R-4***)*

Z-R-4 was prepared as above with **R-3** (438.3 mg, 1.5 mmol), tributyltin hydride (1.51 g, 5.2 mmol) and HMPA (5 mL) to afford **Z-R-4** as a pale oil (314.6 mg, 17.0%). TLC [silica, $CHCl_3/CH_3OH$ (9:1)] R_f = 0.74. ^1H NMR δ 7.63–7.57 (m, 2H), 7.41–7.23 (m, 3H), 6.48–6.35 (pent, 1H), 6.06–6.00 (d, 1H, J = 12.7 Hz), 4.91–4.83 (m, 1H), 3.70 (bs, 1H), 3.03–2.92 (dd, 1H), 2.81–2.70 (dd, 1H), 2.56–2.11 (m, 4H), 2.25 (s, 3H), 2.09–1.60 (m, 4H), 1.57–1.38 (m, 6H), 1.34–1.14 (m, 6H), 0.96–0.80 (m, 15H). ^{13}C NMR δ 174.1, 141.7, 141.3, 133.6, 128.1, 127.6, 125.5, 77.5, 71.9, 52.5, 52.4, 46.3, 30.7, 30.4, 29.2, 27.4, 13.8, 10.3. HPLC analysis: retention time = 11.5 min. $[\alpha]^D$ = −18.59° ($CHCl_3$, c = 39.0 mg/mL).

*2.2.8. E-(R)-1-Methylpiperidin-4-yl α-hydroxy-α-(1-iodo-1-propen-3-yl)-α-phenylacetate (***E-R-1***)*

A solution of **E-R-4** (535.8 mg, 0.9 mmol) in $CHCl_3$ (25 mL) was stirred and a 0.3M $I_2/CHCl_3$ solution was added dropwise until the color of iodine persisted. The resultant solution was stirred at room temperature for 2.5 h, diluted with $CHCl_3$ (100 mL) and washed with a 10% sodium bisulfite solution (50 mL). The $CHCl_3$ solution was dried over anhydrous $MgSO_4$ and evaporated to dryness to afford a pale solid. The product was purified by gravity column chromatography [silica, $CHCl_3/CH_3OH/NH_4OH$ (96:3:1)] to afford **E-R-1** as a pale solid (261.4 mg, 67.7%). Mp: 102–4°C. TLC [silica, $CHCl_3/CH_3OH$ (9:1)] R_f = 0.55. ^1H NMR δ 7.59–7.55 (m, 2H), 7.37–7.25 (m, 3H), 6.58–6.46 (pent, 1H), 6.22–6.15 (d, 1H, J = 14.6 Hz), 4.89–4.81 (m, 1H), 3.95 (bs, 1H), 2.99–2.88 (dd, 1H), 2.75–2.65 (dd, 1H), 2.64–2.32 (m, 4H), 2.25 (s, 3H), 1.99–1.88 (m, 2H), 1.82–1.60 (m, 2H). ^{13}C NMR δ 173.3, 140.8, 139.9, 128.2, 127.9, 125.2, 79.0, 77.4, 72.2, 52.4, 46.1, 45.9, 30.7, 30.3. $[\alpha]^D$ = −31.95° ($CHCl_3$, c = 39.8 mg/mL). HPLC analysis: retention time = 7.0 min. Anal. ($C_{17}H_{22}INO_3$): Calcd: C 49.17, H 5.34, N 3.37; Found: C 49.23, H 5.45, N 3.40.

*2.2.9. E-(S)-1-Methylpiperidin-4-yl α-hydroxy-α-(1-iodo-1-propen-3-yl)-α-phenylacetate (***E-S-1***)*

E-S-1 was prepared as above with **E-S-4** (713.2 mg, 1.2 mmol) to afford the product as a pale solid (524.5 mg, 71.7%). Mp: 104–5°C. TLC [silica, $CHCl_3/CH_3OH$ (9:1)] R_f = 0.36. ^1H NMR δ 7.60–7.54 (m, 2H), 7.40–7.28 (m, 3H), 6.61–6.47 (pent, 1H), 6.23–6.16 (d, 1H, J = 14.5 Hz), 4.88–4.82 (m, 1H), 3.90 (bs, 1H), 3.00–2.89 (dd, 1H), 2.76–2.65 (dd, 1H), 2.60–2.11 (m, 2H), 2.25 (s, 3H), 2.00–1.60 (m, 6H). ^{13}C NMR δ 173.4, 140.8, 140.0, 128.2, 127.9, 125.3, 79.1, 77.4, 72.4, 52.6, 52.5, 46.1, 46.0, 30.8, 30.4. $[\alpha]^D$ = +32.26° ($CHCl_3$, c = 31.8 mg/mL). HPLC analysis: retention time = 7.0 min. Anal. ($C_{17}H_{22}INO_3$) Calcd: C 49.17, H 5.34, N 3.37; Found: C 49.49, H 5.46, N 3.40.

*2.2.10. Z-(S)-1-Methylpiperidin-4-yl α-hydroxy-α-(1-iodo-1-propen-3-yl)-α-phenylacetate (***Z-S-1***)*

Z-S-1 was prepared as above with **Z-S-4** (239.6 mg, 0.4 mmol) to afford the product as a pale oil (147.2 mg, 86.5%). TLC [silica, $CHCl_3/CH_3OH$ (9:1)] R_f = 0.34. ^1H NMR δ 7.64–7.56 (m, 2H), 7.41–7.27 (m, 3H), 6.38–6.22 (m, 2H), 4.87–4.81 (m, 1H), 4.10 (bs, 1H), 3.14–3.03 (dd, 1H), 2.91–2.80 (dd, 1H), 2.62–2.52 (m, 1H), 2.40–2.10 (m, 2H), 2.24 (s, 3H), 1.95–1.64 (m, 4H). ^{13}C NMR δ 173.8, 140.9, 135.6, 128.1, 127.8, 125.4, 85.3, 77.2, 72.2, 52.3, 52.2, 46.1, 44.9, 30.5, 30.2. $[\alpha]^D$ = +15.41° ($CHCl_3$, c = 24.4 mg/

mL). HPLC analysis: retention time = 7.0 min. Anal. ($C_{17}H_{22}INO_3$) Calcd: C 49.17, H 5.34, N 3.37; Found: C 49.77, H 5.55, N 3.20.

*2.2.11. Z-(R)-1-Methylpiperidin-4-yl α-hydroxy-α-(1-iodo-1-propen-3-yl)-α-phenylacetate (***Z-R-1**)

Z-R-1 was prepared as above with **Z-R-4** (314.6 mg, 0.5 mmol) to afford **Z-R-1** as a pale oil (165.9 mg, 74.0%). TLC [silica, $CHCl_3/CH_3OH$ (9:1)] R_f = 0.36. ^1H NMR δ 7.64–7.58 (m, 2H), 7.41–7.29 (m, 3H), 6.39–6.22 (m, 2H), 4.87–4.82 (m, 1H), 4.00 (bs, 1H), 3.15–3.04 (dd, 1H), 2.91–2.80 (dd, 1H), 2.63–2.53 (m, 1H), 2.41–2.11 (m, 2H), 2.25 (s, 3H), 1.96–1.58 (m, 4H). ^{13}C NMR δ 173.8, 140.8, 135.5, 128.2, 127.9, 125.4, 85.3, 77.2, 72.3, 72.2, 52.3, 52.2, 46.1, 44.9, 30.6, 30.2. $[\alpha]^D = -14.81°$ ($CHCl_3$, c = 30.9 mg/mL). HPLC analysis: retention time = 7.0 min. Anal. ($C_{17}H_{22}INO_3$) Calcd: C 49.17, H 5.34, N 3.37; Found: C 49.99, H 5.40, N 3.20.

*2.2.12. Iodine-125-E-(R)-1-methylpiperidin-4-y α-hydroxy-α-(1-iodo-1-propen-3-yl)-α-phenylacetate (***[I-125]-E-R-1**)

An ethanolic solution of **E-R-4** (1 mg/mL, 100 μL), 0.1 N HCl (200 μL) and an ethanolic sodium iodine-125 solution (2.9 mCi in 100 μL of 0.1 M NaOH and 100 μL of ethanol) were added to a 3 mL vial. A freshly prepared 3% H_2O_2 solution (50 μL) was added, the vial sealed, and the solution stirred at room temperature for 30 min. A 10% sodium bisulfite solution (500 μL) was then added, stirred 1 min, and a saturated $NaHCO_3$ solution (1.0 mL) slowly added. The resultant solution was transferred to a syringe containing a C18 Sep Pak. The reaction vial was rinsed with CH_3CN (100 μL) and water (1.0 mL) and these rinses transferred to the syringe. The volume in the syringe was brought up to 10 mL with water and the solution passed through the Sep Pak. The Sep Pak was washed with water (2 × 4 mL) followed by CH_3CN (0.25 mL). The crude radioiodinated product was removed from the Sep Pak with CH_3CN (2 mL) followed by $CHCl_3$ (5 mL) and evaporated to dryness under a stream of nitrogen. The residue was taken up in the HPLC solvent (300 μL) and the product was purified by normal phase HPLC. The HPLC eluent was collected in 1 min increments and the fractions containing the product were pooled together and evaporated under nitrogen to afford 2.2 mCi of **[I-125]-E-R-1** (74.5%) with a specific activity of >800 mCi/μmol and a radiochemical purity >97% determined by HPLC and RTLC analysis, respectively. **[I-125]-E-R-1** was analyzed by comparing the TLC and HPLC mobility to IPIP and in both cases **[I-125]-E-R-1** co-chromatographed with the standard. The specific activity was determined by measurement of the UV absorbance peak (254 nm) corresponding to IPIP and comparing the UV absorbance to a standard curve relating mass to UV absorbance.

*2.2.13. Iodine-125-E-(S)-1-methylpiperidin-4-yl α-hydroxy-α-(1-iodo-1-propen-3-yl)-α-phenylacetate (***[I-125]-E-S-1**)

[I-125]-E-S-1 was prepared in the same manner as above to afford the product in 69.2% radiochemical yield.

*2.2.14. Iodine-125-Z-(R)-1-methylpiperidin-4-yl α-hydroxy-α-(1-iodo-1-propen-3-yl)-α-phenylacetate (***[I-125]-Z-R-1**)

[I-125]-Z-R-1 was prepared in the same manner as above to afford the product in 53.6% radiochemical yield.

*2.2.15. Iodine-125-Z-(S)-1-methylpiperidin-4-yl α-hydroxy-α-(1-iodo-1-propen-3-yl)-α-phenylacetate (***[I-125]-Z-S-1**)

[I-125]-Z-S-1 was prepared in the same manner as above to afford the product in 86.5% radiochemical yield.

2.3. In vitro binding assays

The K_i values for the IPIP stereoisomers were determined by competitive ligand-binding assay with [H-3]-scopolamine as the radiotracer. Competition curves were generated with 12 concentrations of unlabeled compounds: 10^{-12}-10^{-6} M. The various stereoisomers of IPIP were individually dissolved in 100% ethanol and added to 4 mL of tris(hydroxymethyl)aminomethane-buffer (10 mM, pH 7.4) 0.9% saline containing 2.5×10^{-10} M [H-3]-scopolamine at a final concentration of 0.5% ethanol. Aliquots (0.1 mL) of cell membranes were added, the mixture was vortex followed by incubation at 30°C for 2 h. The incubation mixture was rapidly filtered on a GF/C filter paper. The filter was washed with 15 mL of ice cold saline, air-dried, placed in Cytoscint scintillation cocktail (ICN Biomedicals, Inc.), and counted for 2 min each. Data was analyzed with the GraphPad Prism program (San Diego, CA) and K_i values were obtained from a single determination.

2.4. Biodistribution studies

The animal care and use procedures were in accordance with the Guide for the Care and Use of Laboratory Animals and the Animal Welfare Act and were approved by the Oak Ridge National Laboratory Animal Care and Use Committee (ACUC). For these studies, the individual [I-125]-IPIP isomers was dissolved in ethanol and an aliquot (100 μL) was transferred to a vial, 0.1 N HCl solution added (100

Table 1
In vitro M_1 and M_2 binding affinity of IPIP stereoisomers (K_i, nM)

Receptor subtype	Scopolamine (reference)	Stereoisomer of IPIP (**1**)			
		E-R	E-S	Z-R	Z-S
M_1	0.93	3.72	1.10	0.18	0.06
M_2	0.86	10.37	0.93	0.66	0.05

Table 2
In vivo biodistribution of Z-S-IPIP in female rats (n = 5)

Organ	Percent injected dose/gram (±S.D.)					
	15 min	30 min	60 min	120 min	180 min	240 min
Blood	0.41 ± 0.08	0.43 ± 0.07	0.39 ± 0.03	0.37 ± 0.04	0.39 ± 0.04	0.32 ± 0.03
Liver	1.31 ± 0.27	1.25 ± 0.06	1.12 ± 0.05	0.84 ± 0.07	0.71 ± 0.04	0.49 ± 0.03
Kidney	2.42 ± 0.31	2.13 ± 0.19	1.42 ± 0.03	0.77 ± 0.03	0.57 ± 0.07	0.42 ± 0.02
Heart	7.25 ± 1.48	5.97 ± 0.50	3.62 ± 0.26	1.90 ± 0.42	1.05 ± 0.07	0.78 ± 0.10
Lung	5.76 ± 0.80	3.94 ± 0.37	2.40 ± 0.17	1.30 ± 0.06	0.89 ± 0.05	0.69 ± 0.09
Thyroid[a]	0.14 ± 0.08	0.24 ± 0.11	0.52 ± 0.27	1.20 ± 0.75	1.76 ± 0.63	2.13 ± 1.09
Cerebellum	2.68 ± 0.64	2.30 ± 0.21	2.25 ± 0.29	1.85 ± 0.18	1.23 ± 0.05	0.90 ± 0.06
Medulla	2.86 ± 0.63	2.99 ± 0.29	3.01 ± 0.30	2.62 ± 0.34	2.44 ± 0.23	1.96 ± 0.16
Pons	3.04 ± 0.82	3.32 ± 0.26	3.42 ± 0.53	3.64 ± 0.44	3.40 ± 0.63	3.17 ± 0.15
Cortex	4.75 ± 0.83	5.17 ± 0.69	4.94 ± 0.34	5.50 ± 0.66	5.08 ± 0.38	5.26 ± 0.40
Striatum	3.62 ± 0.83	4.13 ± 0.62	3.80 ± 0.30	4.24 ± 0.74	4.16 ± 0.22	4.11 ± 0.38
Hippocampus	3.01 ± 0.56	3.04 ± 0.39	3.33 ± 0.35	3.77 ± 0.46	3.59 ± 0.25	3.46 ± 0.36
Thalamus	3.37 ± 1.00	3.57 ± 0.42	3.53 ± 0.43	4.23 ± 0.72	3.70 ± 0.26	3.70 ± 0.34
Superior colliculi	3.71 ± 0.90	3.63 ± 0.45	3.84 ± 0.58	4.34 ± 0.51	3.77 ± 0.34	3.51 ± 0.37
Inferior colliculi	3.98 ± 0.93	3.87 ± 0.28	4.21 ± 0.63	4.48 ± 0.64	3.81 ± 0.31	3.34 ± 0.29

[a] Percent injected dose.

μL), and the volume brought up to 10 mL with sterile normal saline. Following filtration through a 0.22 μ Millipore filter into a sterile injection vial, the solution was administered by intravenous injection (0.5 mL) into a lateral tail vein of metophane-anesthetized female rats (n = 5 rats/group, 4–6 μCi). The rats were monitored as they recovered from anesthesia and allowed food and water during the course of the experiment. The rats were then anesthetized and euthenized by cervical dislocation at designated times post injection of the radioiodinated ligand. The various organs were removed, rinsed with saline, blotted dry, and weighed in tarred vials. Blood samples were obtained from the thoracic cavity after removal of the heart. The brains were removed, placed on a cold surface (ice) and immediately dissected into the various regions. The tissues were weighed and counted in a Packard Minaxi 5000 auto sodium iodide gamma counter.

For blocking studies with E-R- and Z-S-IPIP, groups of rats (n = 5) were anesthetized as above and pretreated with a saline solution (0.5 mL) of the oxalate salt of R-QNB (3 mg/kg) 30 min or 1 h prior to injection of the [I-125]-Z-S- or E-R-IPIP, respectively. As a control, a group of animals (n = 5) were injected with only E-R- or Z-S-IPIP, respectively. The rats were anesthetized and euthenized by cervical dislocation 2 h post injection of Z-S-IPIP or 3 h post-injection of E-R-IPIP. The various organs were removed and treated as described above.

2.5. Tissue extraction and analysis

The chilled global brain and heart were finely minced in a watch glass and homogenized for 3 min in a $CHCl_3$/CH_3OH solution (10 mL, 2:1 v/v) by the traditional Folch technique as described previously using a loose fitting Pot-

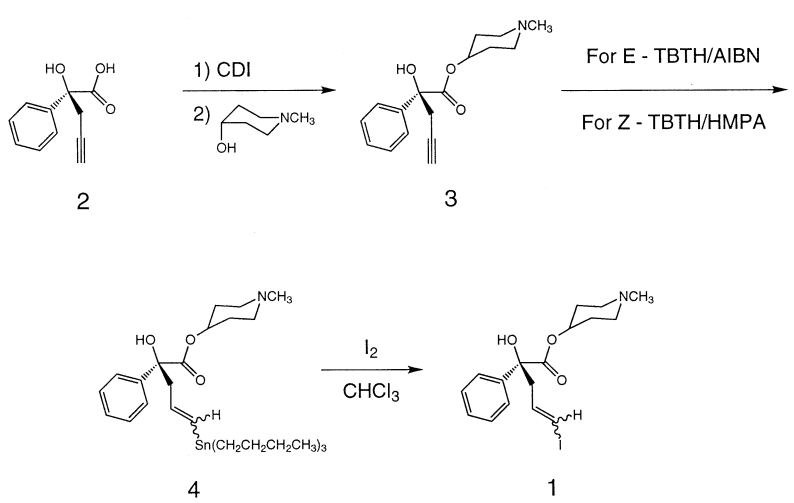

Scheme 1. Activated Ester Approach for the Synthesis of IPIP.

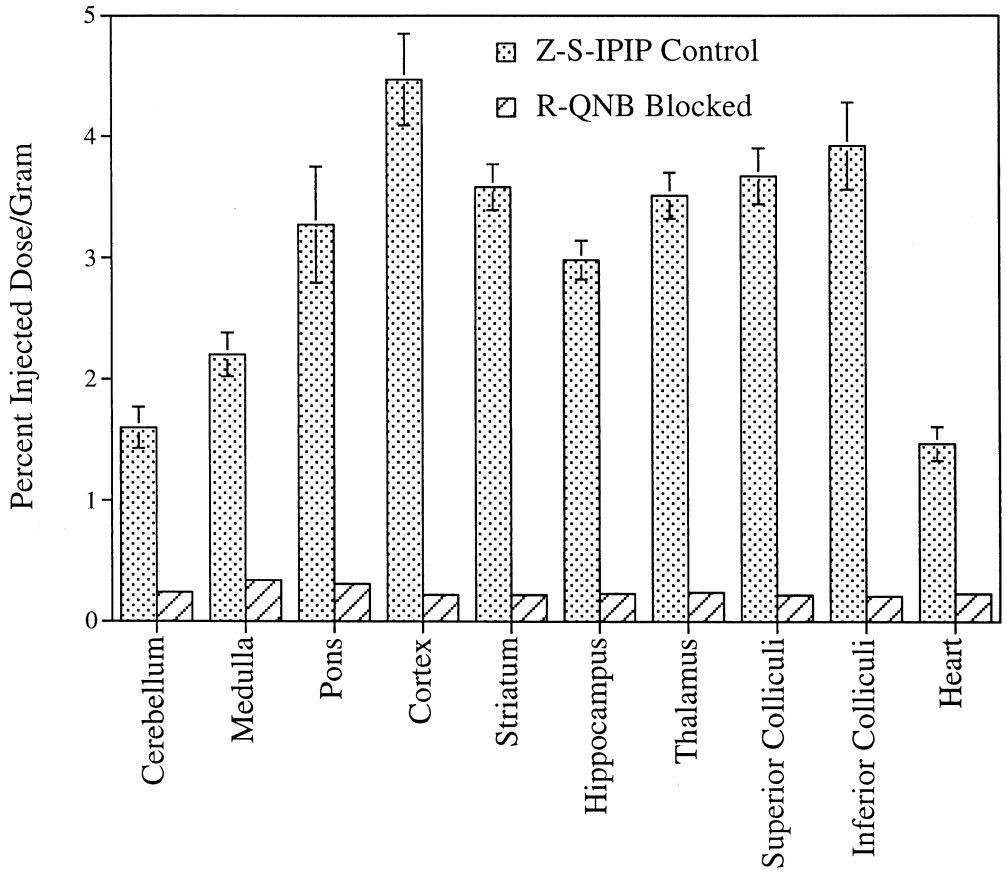

Fig. 2. *In vivo* blocking study with R-QNB (3 mg/kg, 0.5 h pre-injection) in female fischer rats at 2 h post-injection of [I-125]-Z-S-IPIP (n = 5).

ter-Elmejahn ground glass homogenizer [25]. The individual organic extracts were filtered into centrifuge tubes and the filter paper washed with $CHCl_3$ (1 mL). The filtrates were thoroughly mixed with normal saline (2 mL) and centrifuged at low speed for 10 min to separate the organic and aqueous layers. The organic layer was carefully removed with a pipette and filtered through a short column of anhydrous sodium sulfate and evaporated to dryness under a stream of argon. The organic fraction, aqueous fraction and filter paper/pellet combination were counted. The organic residues were dissolved in $CHCl_3$ (0.5 mL) and analyzed for Z-S-IPIP by TLC analysis ($CHCl_3/CH_3OH$ [8.5: 1.5], R_f = 0.40).

3. Results

3.1. Synthesis

The four stereoisomers of IPIP were prepared *via* a stereoselective synthesis utilizing *cis*-(2R,5R)- or (2S,5S)-2-(tert-butyl)-5-phenyl-5-(1-propyn-3-yl)-1,3-dioxlan-4-one [24]. An activated ester approach was utilized for the esterification of α-hydroxy-α-phenyl-α-(1-propyn-3-yl)acetic acid (**2**) with 1-methyl-4-hydroxypiperidine to afford the desired propynyl intermediate (**3**) (Scheme 1) [18,37]. The tributylstannyl intermediates (**4**) were prepared by the treatment of the propynyl intermediate (**3**) with tributyltin hydride. Treatment of **3** with a slight excess of tributlytin hydride in the presence of the radical initiator AIBN afforded the E isomers. Treatment of **3**

Table 3
In vivo biodistribution of Z-R-IPIP in female rats (n = 5)

Organ	Percent injected dose/gram (±S.D.)		
	15 min	120 min	240 min
Blood	0.60 ± 0.08	0.52 ± 0.08	0.43 ± 0.04
Liver	1.04 ± 0.04	0.40 ± 0.06	0.26 ± 0.03
Kidney	1.94 ± 0.23	0.61 ± 0.10	0.33 ± 0.06
Heart	1.62 ± 0.14	0.39 ± 0.03	0.24 ± 0.02
Lung	6.36 ± 1.09	1.15 ± 0.25	0.54 ± 0.04
Thyroid[a]	0.20 ± 0.07	1.22 ± 0.57	3.44 ± 1.44
Cerebellum	1.93 ± 0.18	0.30 ± 0.06	0.12 ± 0.02
Medulla	2.37 ± 0.21	0.71 ± 0.14	0.31 ± 0.06
Pons	3.18 ± 0.30	1.55 ± 0.19	0.77 ± 0.13
Cortex	4.79 ± 0.23	3.57 ± 0.63	2.16 ± 0.15
Striatum	3.81 ± 0.24	3.54 ± 0.57	2.28 ± 0.19
Hippocampus	3.54 ± 0.14	2.82 ± 0.48	1.96 ± 0.15
Thalamus	3.61 ± 0.20	2.09 ± 0.33	1.02 ± 0.05
Superior colliculi	3.73 ± 0.29	1.26 ± 0.21	0.58 ± 0.05
Inferior colliculi	3.72 ± 0.28	1.01 ± 0.13	0.48 ± 0.05

[a] Percent injected dose.

Table 4
In vivo biodistribution of E-R-IPIP in female rats (n = 5)

Organ	Percent injected dose/gram (±S.D.)					
	15 min	30 min	60 min	120 min	180 min	240 min
Blood	0.51 ± 0.01	0.50 ± 0.02	0.51 ± 0.06	0.44 ± 0.03	0.31 ± 0.03	0.31 ± 0.03
Liver	1.20 ± 0.07	0.92 ± 0.04	0.70 ± 0.07	0.51 ± 0.05	0.38 ± 0.03	0.32 ± 0.02
Kidney	1.87 ± 0.12	1.31 ± 0.13	1.06 ± 0.06	0.61 ± 0.06	0.36 ± 0.03	0.31 ± 0.03
Heart	0.78 ± 0.08	0.57 ± 0.03	0.40 ± 0.02	0.25 ± 0.02	0.15 ± 0.02	0.13 ± 0.01
Lung	6.49 ± 1.03	3.31 ± 0.29	2.16 ± 0.23	0.94 ± 0.15	0.50 ± 0.07	0.40 ± 0.04
Thyroid[a]	0.26 ± 0.17	0.42 ± 0.29	1.15 ± 0.42	1.13 ± 0.64	2.77 ± 1.65	3.77 ± 2.82
Cerebellum	1.46 ± 0.16	0.84 ± 0.12	0.39 ± 0.02	0.18 ± 0.02	0.09 ± 0.01	0.06 ± 0.01
Medulla	1.90 ± 0.30	1.33 ± 0.29	0.83 ± 0.08	0.31 ± 0.03	0.21 ± 0.05	0.08 ± 0.04
Pons	1.72 ± 0.20	1.68 ± 0.54	0.63 ± 0.04	0.73 ± 0.24	0.15 ± 0.04	0.23 ± 0.09
Cortex	2.28 ± 0.12	1.80 ± 0.11	0.99 ± 0.04	0.77 ± 0.06	0.39 ± 0.03	0.36 ± 0.04
Striatum	2.17 ± 0.05	1.79 ± 0.16	0.97 ± 0.04	0.76 ± 0.04	0.40 ± 0.03	0.41 ± 0.03
Hippocampus	2.04 ± 0.19	1.79 ± 0.24	0.96 ± 0.05	0.66 ± 0.06	0.33 ± 0.01	0.34 ± 0.03
Thalamus	2.24 ± 0.23	1.69 ± 0.22	0.82 ± 0.01	0.58 ± 0.03	0.24 ± 0.03	0.21 ± 0.02
Superior colliculi	1.91 ± 0.17	1.22 ± 0.30	0.62 ± 0.05	0.36 ± 0.07	0.14 ± 0.03	0.10 ± 0.03
Inferior colliculi	1.85 ± 0.17	1.04 ± 0.21	0.54 ± 0.03	0.36 ± 0.05	0.14 ± 0.02	0.10 ± 0.02
Rest of brain	1.79 ± 0.13	1.38 ± 0.10	0.73 ± 0.03	0.51 ± 0.05	0.26 ± 0.02	0.23 ± 0.02

[a] Percent injected dose.

with an excess of tributyltin hydride in HMPA afforded the Z-isomers. Subsequent treatment of the individual E-and Z-**4** stereoisomers with iodine afforded the IPIP stereoisomers. HPLC analysis of the IPIP stereoisomers prepared *via* this route showed the E isomers contained approximately 4–5% of the respective Z isomers and the Z isomers with approximately 7–8% of the respective E isomers.

3.2. In vitro binding assay

Single determination of the *in vitro* binding affinity of the individual IPIP stereoisomers utilizing cloned human M_1 and M_2 receptor subtypes was determined using [H-3]-methylscopolamine as the reference ligand (Table 1). The IPIP stereoisomers bound with nanomolar affinity to mAChR with the R-isomers demonstrating a low subtype selectivity for the M_1 subtype (3 to 5 fold) over the M_2 subtype and the S isomers demonstrating a non-subtype selectivity.

3.3. Radiolabeling

Radioiodination of the individual IPIP stereoisomers was accomplished utilizing a freshly prepared 3% hydrogen peroxide solution as the oxidant and purified *via* HPLC. The individual [I-125]IPIP isomers were obtained in high radiochemical yield (74.4 ± 14.8%, n = 5), high radiochemical

Table 5
In vivo biodistribution of E-S-IPIP in female rats (n = 5)

Organ	Percent injected dose/gram (±S.D.)					
	15 min	30 min[a]	60 min	120 min	180 min	240 min
Blood	0.27 ± 0.02	0.25 ± 0.02	0.28 ± 0.02	0.29 ± 0.03	0.25 ± 0.02	0.25 ± 0.03
Liver	2.97 ± 0.25	3.00 ± 0.68	3.35 ± 0.14	2.69 ± 0.13	1.64 ± 0.07	1.41 ± 0.14
Kidney	2.91 ± 0.43	2.08 ± 0.22	1.74 ± 0.10	1.06 ± 0.12	0.65 ± 0.08	0.52 ± 0.05
Heart	1.19 ± 0.20	0.78 ± 0.06	0.60 ± 0.07	0.36 ± 0.03	0.34 ± 0.06	0.21 ± 0.02
Lung	4.67 ± 0.66	2.99 ± 0.32	1.53 ± 0.13	0.89 ± 0.03	0.56 ± 0.05	0.45 ± 0.03
Thyroid[b]	0.11 ± 0.05	0.22 ± 0.09	0.41 ± 0.16	0.84 ± 0.34	0.99 ± 0.64	1.78 ± 0.99
Cerebellum	1.78 ± 0.24	1.30 ± 0.39	1.07 ± 0.12	0.62 ± 0.06	0.35 ± 0.03	0.23 ± 0.02
Medulla	1.60 ± 0.19	1.75 ± 0.33	1.00 ± 0.11	0.63 ± 0.16	0.52 ± 0.05	0.33 ± 0.02
Pons	2.13 ± 0.36	1.54 ± 0.46	1.05 ± 0.12	0.71 ± 0.06	0.56 ± 0.06	0.32 ± 0.05
Cortex	2.88 ± 0.33	1.78 ± 0.38	1.36 ± 0.08	0.81 ± 0.07	0.50 ± 0.04	0.39 ± 0.02
Striatum	2.70 ± 0.27	1.76 ± 0.50	1.34 ± 0.10	0.79 ± 0.08	0.52 ± 0.04	0.38 ± 0.03
Hippocampus	2.32 ± 0.23	1.61 ± 0.47	1.32 ± 0.12	0.80 ± 0.07	0.49 ± 0.05	0.35 ± 0.01
Thalamus	2.44 ± 0.24	1.75 ± 0.48	1.10 ± 0.16	0.69 ± 0.08	0.47 ± 0.04	0.32 ± 0.02
Superior colliculi	2.24 ± 0.24	1.43 ± 0.41	1.10 ± 0.11	0.68 ± 0.06	0.43 ± 0.04	0.29 ± 0.03
Inferior colliculi	2.17 ± 0.23	1.45 ± 0.37	0.99 ± 0.08	0.63 ± 0.05	0.35 ± 0.12	0.27 ± 0.02

[a] 4 rats/group.
[b] Percent injected dose.

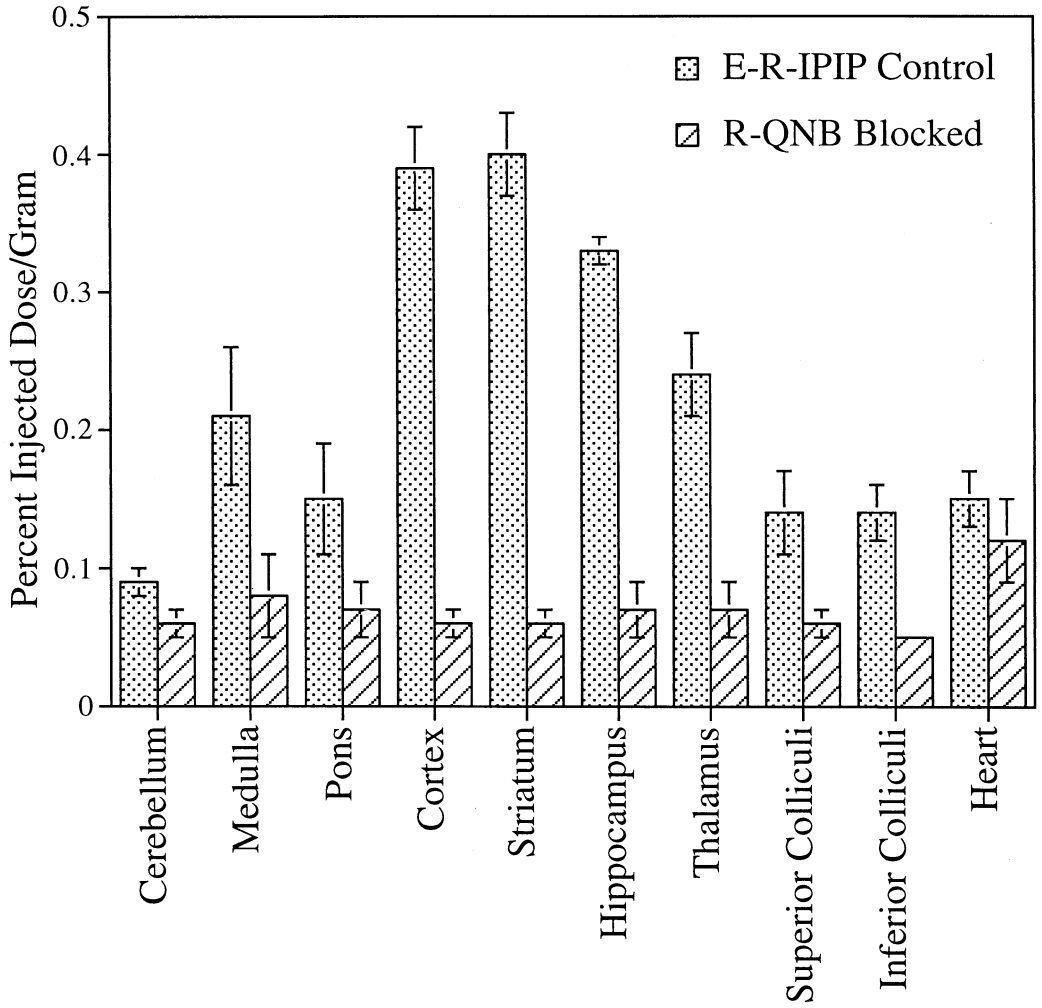

Fig. 3. *In vivo* blocking study with R-QNB (3 mg/kg, 1 h pre-injection) in female fischer rats at 3 h post-injection of [I-125]-E-R-IPIP (n = 5).

purity (>97%), and high specific activity (>800 mCi/μmol) as determined by RTLC and HPLC, respectively.

3.4. In vivo biodistribution

The biodistribution of the four IPIP stereoisomers were investigated in female Fischer rats over 4 h and significant differences in cerebral and cardiac uptake and receptor binding of the various isomers were in agreement with the *in vitro* binding data (Tables 2–5). Z-S-IPIP demonstrated high uptake and significant retention in all cerebral regions studied in addition to a significant cardiac uptake (Table 2). The cerebral and cardiac uptake of radioactivity was blocked > 90% by the pre-injection of R-QNB (3 mg/kg) 30 min prior to the injection of Z-S-IPIP (Fig. 2). Z-R-IPIP demonstrated similar high initial cerebral uptake as compared to Z-S-IPIP but a rapid cerebral clearance from regions containing a high concentration of the M_1 subtype and a significantly higher washout from M_2 rich regions (cerebellum, superior and inferior colliculi, medulla) (Table 3). In addition, Z-R-IPIP did not demonstrate significant cardiac uptake.

The E-isomers demonstrated a slightly lower uptake of cerebral activity as compared to the Z-isomers. At 4 h post-injection, after the measurable uptake in M_2 rich regions was allowed to clear, E-R-IPIP localized in cerebral regions containing a high concentration of the M_1, M_4 subtype (cortex, striatum, hippocampus, thalamus) (Table 4). In addition, the activity in M_1, M_4 rich areas was blocked to the level of non-specific binding following pretreatment of the rat with R-QNB (3 mg/kg) 1 h prior to the injection of E-R-IPIP (Fig. 3). Importantly, at 4 h post-injection, the level of activity remaining in the cerebellum and heart, regions containing primarily the M_2 subtype, was not decreased *via* pretreatment with R-QNB.

E-S-IPIP demonstrated similar initial uptake as compared to E-R-IPIP, however, the cerebral activity was retained for a longer period of time (Table 5).

An *ex vivo* metabolic study was performed utilizing Z-S-IPIP to obtain information concerning the identity of

Table 6
Ex vivo evaluation of Z-S-IPIP in global rat brain and heart tissue (n = 5)

Time (min)	Brain				Heart			
	% Organic fraction	% Aqueous fraction	% Pellet fraction	% IPIP *via* TLC	% Organic fraction	% Aqueous fraction	% Pellet fraction	% IPIP *via* TLC
15	71.5 (±2.7)	2.1 (±0.8)	26.5 (±2.5)	96.6 (±1.7)	70.1 (± 9.3)	4.7 (±0.8)	25.2 (±9.2)	92.1 (±3.2)
30	67.2 (±0.9)	1.9 (±0.6)	31.0 (±1.3)	94.4 (±1.2)	71.3 (±18.8)	6.1 (±1.7)	22.7 (±20.3)	90.8 (±4.5)
60	86.0 (±7.2)	0.9 (±0.4)	13.2 (±6.8)	98.4 (±0.9)	71.6 (±11.2)	6.6 (±0.6)	21.8 (±10.7)	96.7 (±0.6)
240	76.8 (±1.5)	2.8 (±1.1)	20.5 (±1.2)	93.7 (±4.2)	67.1 (±4.4)	10.7 (±1.0)	22.3 (±3.4)	93.7 (±4.2)
480	75.1 (±1.7)	1.3 (±0.7)	23.7 (±1.4)	97.3 (±1.2)	63.2 (±4.3)	12.6 (±1.8)	24.3 (±3.5)	79.2 (±7.2)

the species responsible for cerebral binding (Table 6). Greater than 80% of the global brain activity was extracted into the organic phase and observed to be unmetabolized IPIP (>97%) for up to 8 h post-injection. In addition, >85% of the activity obtained from global heart tissue was extracted in the organic phase and observed to be unmetabolized IPIP. In both analyses approximately 15–20% of the activity from these extractions was associated with the pellet and filter.

4. Discussion

Initial animal and human SPECT imaging studies with IQNP demonstrated important improvements in the development of radioiodinated ligands targeted to the individual mAChR subtypes (i.e. high cerebral uptake, modest subtype selectivity, high binding to M_2 rich tissues) [4,5,22,23,26, 29,30,32]. However, IQNP does not display optimum receptor binding kinetic properties for the evaluation of receptor function [29]. As has been observed for various quinuclidinyl esters, IQNP displays a slow dissociation from the receptor pocket and therefore is not optimal for the development of an appropriate *in vivo* receptor binding model.

Addressing the important issue of receptor binding kinetics, it has been postulated that an improvement in the binding kinetics may be achieved *via* the development of a ligand with a decreased *in vitro* binding affinity (i.e. 1 nM *vs.* 0.01 nM) [36,43]. Therefore the initial modification envisioned for the IQNP structure involved modification of the 3-quinuclidinyl moiety to a 1-methylpiperidin-4-yl moiety, the simplest piperidinyl group.

4.1. Chemistry

The initial synthetic route envisioned for the preparation of IPIP was based on the stereoselective synthesis reported for IQNP (Scheme 2). Transesterification of R-ethyl α-hydroxy-α-(1-propyn-3-yl)-α-phenyl acetate (**5**) with the sodium salt of 4-hydroxy-1-methylpiperidine afforded the desired piperidinyl ester (**3**). Although a single spot was observed *via* TLC analysis following flash column chromatography purification of **3**, NMR analysis indicated the presence of an allenyl analogue, 1-methylpiperidin-4-yl α-(allenyl)-α-hydroxy-α-phenylacetate (**6**) that co-eluted with **3**.

The allenyl compound (**6**) can be postulated to arise from the formation of a conjugated propenyl anion intermediate (**7**) in the presence of base under the harsh reaction condi-

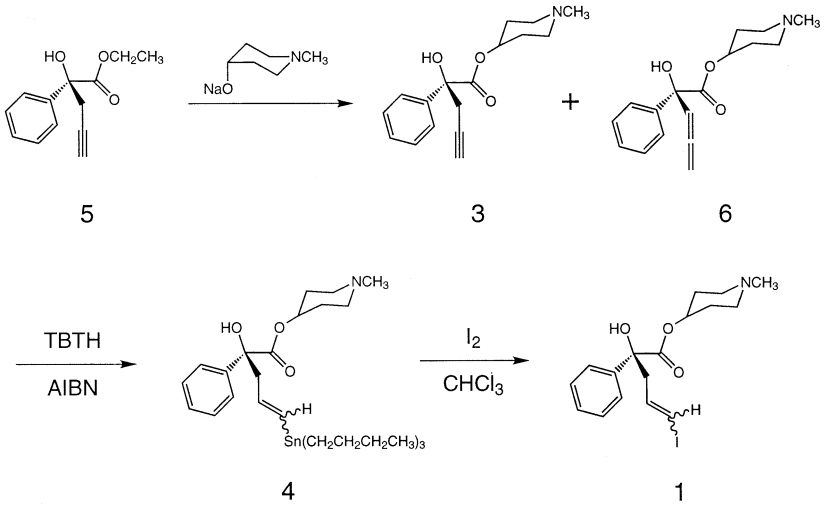

Scheme 2. Transesterification approach for the synthesis of IPIP.

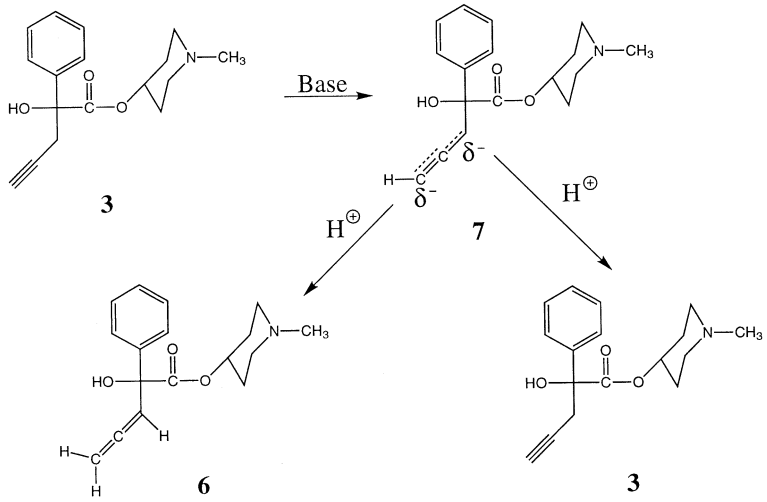

Scheme 3. Proposed formation of allenyl IPIP analogue (**6**).

tions employed for the transesterification (Scheme 3). Subsequent quenching of the reaction *via* the addition of water affords both **3** and **6**.

The mixture of **3** and **6** was subsequently treated with tributyltin hydride in the presence of a slight excess of AIBN to afford (E)-1-methylpipidin-4-yl α-hydroxy-α-phenyl-α-(1-tributylstannyl-1-propen-3-yl)acetate (**4**) in 80% chemical yield (Scheme 4). 1-Methylpiperidin-4-yl α-hydroxy-α-phenyl-α-(3-tributylstannyl-1-propen-3-yl)-acetate (**9**) in which the tributylstannyl moiety was added to the 3 position of the propenyl group was not observed by NMR analysis. Analogous to the formation of the allenyl intermediate, the formation of a conjugated radical intermediate (**8**) can be postulated as an intermediate in the addition of the tributylstannyl moiety. However as previously observed for the preparation of the Z-isomers of IQNP [26], the steric bulk associated with the acetate center exclusively favors the formation of **4**.

Due to the low yield and complex product formation obtained for the transesterification reaction, a one-pot activated ester approach utilizing carbonyldiimidazole (CDI) for the esterification of ethyl α-hydroxy-α-(1-propyn-3-yl)-α-phenylacetic acid (**2**) was investigated (Scheme 1) [18, 37]. The formation of the activated ester proceeded smoothly at room temperature in anhydrous DMF with a 1 to 1 molar equivalent of **2** and CDI. The subsequent reaction of the activated ester with 1-methyl-4-hydroxypiperidine was investigated to optimize the esterification yield (Table 7). An esterification yield of 44% for the desired ester (**3**) was obtained using anhydrous DMF as the solvent and a temperature of 80°C. Although a higher yield of **3** was obtained when the temperature was increased to 110°C, **3** was difficult to purify due to several unidentified impurities.

As reported for the Z-IQNP isomers, the Z-IPIP isomers were also isolated in low yields when the reaction was performed with an excess of tributyltin hydride in HMPA

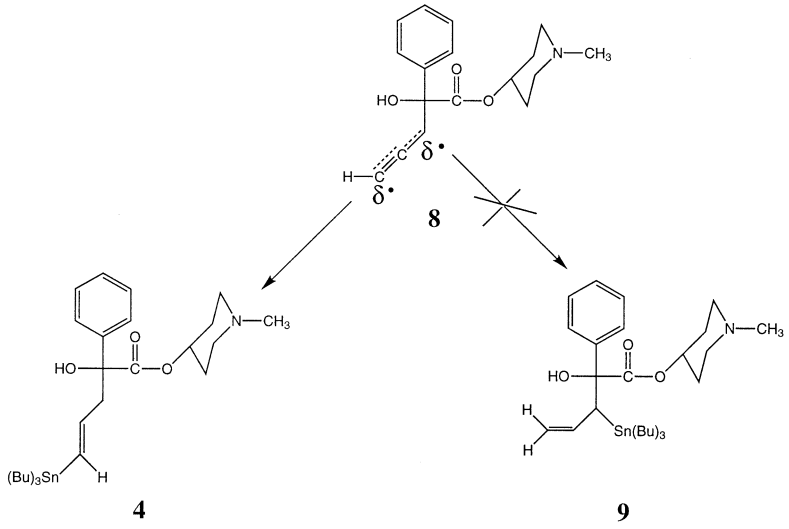

Scheme 4. Proposed radical addition of tributyltin hydride to allenyl IPIP analogue (**6**).

Table 7
Evaluation of solvent and temperature on the esterification of the activated ester of **2** with 1-hydroxy-4-methylpiperidine

Solvent	Temperature	Yield of **3**
THF	Room temperature	12.2 (n = 1)
THF	Reflux	19.1 ± 11.2 (n = 2)
DMF	Room temperature	24.3 (n = 1)
DMF	65°C	42.9 (n = 1)
DMF	70°C	35.2 ± 2.4 (n = 2)
DMF	80°C	44.0 ± 2.7 (n = 3)
DMF	90°C	37.1 ± 23.4 (n = 2)
DMF	110°C	51.7 (n = 1)

1-Hydroxy-4-methylpiperidine (mmol)/activated acid (mmol) = 2.4 ± 1.0.
Reaction time—18 h.

[26]. Use of an aprotic solvent with an excess of tributyltin hydride has been reported to afford high yields of the Z isomer [16], therefore various aprotic solvents were investigated (Table 8). In this study, the solvents and temperatures investigated did not markedly affect the isolated yield of Z-**4** except in the case of acetonitrile which, surprisingly, only the E isomer was isolated in 64% yield. In addition to **E-** and **Z-4**, unreacted **3** was recovered from the reaction mixture to account for >90% of the initial mass of **3**. These results lend further support that the steric bulk at the acetate center is the major influence on the orientation for the addition of the tributylstannyl moiety for this class of compounds.

Treatment of the individual tributylstannyl isomers (**4**) with iodine afforded IPIP with retention of configuration on the vinyl position. Radioiodination of the individual IPIP stereoisomers with retention of configuration was accomplished with the tributylstannyl intermediate (**4**) utilizing a 3% hydrogen peroxide solution as the oxidant.

4.2. Biodistribution

A decrease in the *in vitro* M_1 subtype binding affinity in addition to a decrease in the selectivity of the E-IPIP isomers for the M_1 subtype as compared to E-RR-IQNP was observed (Table 1). The Z-isomers demonstrated a high binding affinity for the M_2 subtype in addition to the M_1 subtype suggesting a non-subtype selectivity with respect to the mAChR subtypes.

Table 8
Evaluation of aprotic solvent and temperature on the formation of the Z-IPIP isomers (**4**)

Solvent	Temperature	% Z-isomer	% E-isomer
Acetonitrile	50°C	0.0	64.7
DMSO	80°C	9.2	12.9
HMPA (n = 2)	50°C	2.6–14.3	7.9–60.1
DMF	50°C	9.5	9.5
DMF (n = 5)	80°C	16.3 ± 5.5	20.8 ± 10.3

Tributyltin hydride (mmol)/**3** (mmol) = 3.5 ± 0.6.
Reaction time—3–5 days.

Biodistribution of the individual IPIP stereoisomers were investigated in female rats and a significant increase in the uptake of the IPIP isomers was observed as compared to that reported for IQNP [26]. The increased cerebral uptake of IPIP can be postulated to result from the decreased lipophilicity of IPIP as compared to IQNP, as observed by HPLC, and allows for an increased diffusion across the intact blood brain barrier.

The biodistribution of cerebral radioactivity for the Z-isomers suggests a non-subtype selective binding in agreement with the *in vitro* binding assays. As observed for Z-RR-IQNP, the Z-IPIP isomers demonstrate slow release from cerebral regions containing a high concentration of the M_1 subtype and a more rapid release from regions containing a high concentration of the M_2 subtype (Tables 2 and 3). Comparing the cerebral binding profile of Z-isomers, a faster global cerebral release of activity associated with Z-R-IPIP may be due to the 3 and 13 fold decrease in the *in vitro* binding affinity for the M_1 and M_2 subtypes, respectively, as compared to Z-S-IPIP.

To confirm that the cerebral and cardiac uptake of Z-S-IPIP was receptor mediated and not solely an indication of non-specific uptake, a receptor blocking study was performed utilizing R-QNB, an established non-subtype selective muscarinic antagonist (Fig. 2). This study demonstrated blocking the receptor sites with R-QNB reduces the level of radioactivity by approximately 90% in all cerebral regions in addition to the heart.

The E isomers demonstrated a lower cerebral and cardiac uptake as compared to the Z-isomers (Tables 4 and 5). In addition, as suggested by the *in vitro* binding assays, the E-isomers demonstrated a higher *in vivo* selectivity for the M_1 subtype over the M_2 subtype. E-R-IPIP showed a more rapid release and cerebral washout from regions containing a high concentration of the M_2 subtype (cerebellum, heart) as compared to E-S-IPIP reflecting the decreased *in vitro* binding affinity for the M_2 subtype.

An analogous blocking study as above with E-R-IPIP was performed to evaluate specific receptor binding (Fig 3). Pretreatment with R-QNB significantly reduced the cerebral level of activity by 53 to 85% at 3 hours post-injection of [I-125]-E-R-IPIP in all regions evaluated except for the cerebellum and heart, two regions containing a high concentration of the M_2 subtype. Since R-QNB is non-subtype selective, a decrease in level of activity would be expected if E-R-IPIP was binding to these regions. Therefore the remaining radioactivity is measure of the non-specific binding in these tissues. This study demonstrated E-R-IPIP binds to cerebral regions containing a high concentration of the M_1 subtype after allowing the initial cerebral binding to the M_2 subtype to clear.

An *ex vivo* metabolism study utilizing Z-S-IPIP was performed to evaluate the species responsible for binding at the receptor site (Table 6). In global brain tissue, approxi-

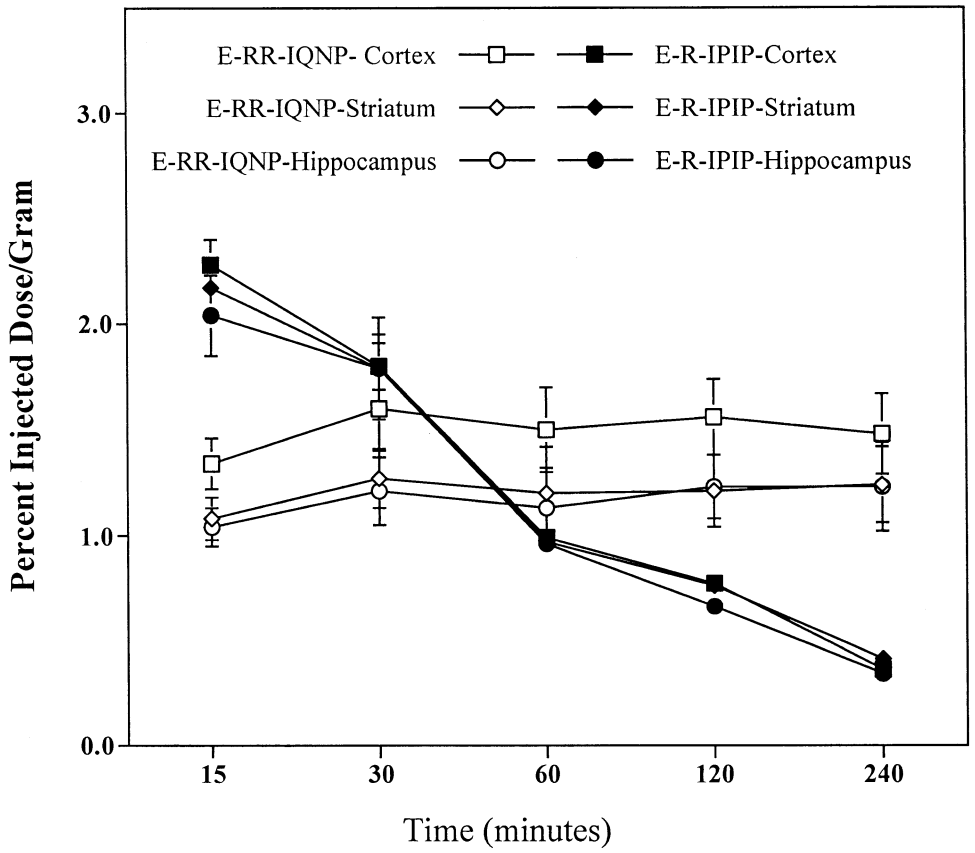

Fig. 4. Comparison of the *in vivo* uptake and retention of activity of E-R-IPIP and E-RR-IQNP in female rats (n = 5).

mately 75% of the activity up to 8 h post-injection was extracted into the organic phase and identified as unmetabolized Z-S-IPIP (>93%) *via* TLC analysis. In global heart tissue, an analogous result was observed up to 4 h post-injection. However, at 4 h post-injection, the appearance of undetermined metabolites was observed and at 8 h post injection, the level of unmetabolized Z-S-IPIP in the organic fraction was decreased to 80%.

An important rationale for the modification of IQNP was to decrease the binding affinity allowing the accurate and reproducible modeling of the receptor ligand binding parameters, i.e., on- and off-rate, to be constructed. IQNP and IQNB both demonstrate an unfavorable slow release from the receptor site that prohibits a clear distinction of receptor binding from blood flow and thus prohibiting the modeling of these important parameters. These preliminary results presented in these studies demonstrates E-R-IPIP shows an improved *in vitro* binding affinity, cerebral uptake, faster release and washout from the receptor site as compared to E-RR-IQNP (Fig. 4).

5. Conclusion

We have evaluated 1-methylpiperidin-4-yl α-hydroxy-α-(1-iodo-1-propen-3-yl)-α-phenylacetate (IPIP, Fig. 1) as a potential molecular probe targeted to the muscarinic receptor complex. The individual stereoisomers were synthesized *via* a stereoselective intermediate in >95% enantiomeric excess and radiolabeled with iodide-125 *via* a tributylstannyl intermediate in a radiochemical yield of 74.4% ($\pm$14.8, n = 5), specific activity >800 mCi/μmol, and a radiochemical purity >97% following HPLC purification. *In vitro*, the IPIP isomers demonstrated high binding affinity with E-R-IPIP demonstrating a modest M_1 to M_2 subtype selectivity (approximately 3 to 1). *In vivo* biodistribution studies in female Fischer rats demonstrated significant initial cerebral uptake for the IPIP stereoisomers. The Z-IPIP isomers demonstrated a high global cerebral uptake suggesting non-subtype selective uptake during the time course of the study. In contrast, E-R-IPIP, after allowing the low but measurable uptake in M_2 rich areas to clear, demonstrated retention of activity in M_1 and M_4 rich cerebral regions. An *ex vivo* metabolism study demonstrated Z-S-IPIP effectively crossed the blood-brain-barrier and was stable at the receptor site with an absence of radiolabeled metabolites competing at the receptor site. The facile radiolabeling, high cerebral uptake, favorable binding kinetics, and *in vivo* stability demonstrate the potential utilization of the stereoisomers of IPIP for imaging of the muscarinic receptor *via* SPECT.

Acknowledgments

The authors thank Dr. D. DeHaven-Hudkins and Dr. R. Reba for assistance with the *in vitro* studies. Research was supported at Oak Ridge National Laboratory, managed by UT-Battelle, LLC, for the United States Department of Energy, under contract DE-AC05-00OR22725.

References

[1] M. Asahina, H. Shinotoh, Muscarinic cholinergic receptor imaging of parkinsonian brains using ^{11}C-NMPB and PET, Nippon Rinsho 55 (1997) 233–237.

[2] M. Asahina, H. Shinotoh, K. Hirayama, T. Suhara, F. Shishido, O. Inoue, Y. Tateno, Hypersensitivity of cortical muscarinic receptors in Parkinson's disease demonstrated by PET, Acta Neurol. Scand. 91 (1995) 437–443.

[3] I. Aubert, D.M. Araujo, D. Cecyre, Y. Robitaille, S. Gauthier, R. Quirion, Comparative alterations of nicotinic and muscarinic binding sites in Alzheimer's and Parkinson's disease, J. Neurochem. 58 (1992) 529–541.

[4] K.A. Bergstrom, C. Halldin, J. Hiltunen, C.G. Swahn, H. Ito, N. Ginovert, H. Hall, D.W. McPherson, F.F. Knapp Jr., S. Larsson, P.O. Schnell, L. Farde, I-125 and I-123-labeled E-(-,-)-IQNP: Potential radioligand for visualization of M_1 acetylcholinergic receptors in brain. Determination of metabolites using HPLC, Nucl. Med. Biol. 25 (1998) 209–214.

[5] K. Bergstrom, C. Halldin, A. Savonen, Y. Okubo, J. Hiltunen, K. Nobuhara, C.G. Swahn, P. Karlsson, D.W. McPherson, F.F. Knapp Jr., S. Larsson, P.O. Schnell, L Farde, Iodine-123 labelled Z-R,R-IQNP: A potential radioligand for visualization of M_1 and M_2 muscarinic acetylcholine receptors in Alzheimer's disease, Eur. J. Nucl. Med. 26 (1999) 1482–1485.

[6] K.L. Boundy, L.R. Barnden, C.C. Rowe, M. Reid, M. Kassiou, A.G. Katsifis, R.M. Lambrecht, Human dosimetry and biodistribution of iodine-123-iododexetimide: A SPECT imaging agent for cholinergic muscarinic neuroreceptors, J. Nucl. Med. 36 (1995) 1332–1338.

[7] K.L. Boundy, C.C. Rowe, A.B. Black, M.I. Kitchener, L.R. Barnden, R. Sebben, A. Kneebone, M. Kassiou, A. Katsifis, R. Lambrecht, Localization of temporal lobe epileptic foci with iodine-123 iododexetimide cholinergic neuroreceptor single-photon emission computed tomography, Neurology 47 (1996) 1015–1020.

[8] W.F. Breeden, D.M. Hamby, J.E. Carey, K.F. Eckerman, D.W. McPherson, F.F. Knapp Jr., *In vivo* biodistribution of ^{125}I-IPIP and internal dosimetry of ^{123}I-IPIP radioiodinated agents selective to the muscarinic acetylcholinergic receptor complex, Med. Physics 27 (2000) 778–786.

[9] N.J. Buckley, T.I. Bonner, C.M. Buckley, M.R. Brann, Antagonist binding properties of five cloned muscarinic receptors expresses in CHO-K_1 cells, Mol. Pharmacol. 35 (1989) 469–476.

[10] J.J. Claus, E.A. Dubois, J. Booij, J. Habraken, J.C. de Munck, M. van Herk, B. Verbeeten, E.A. van Royen, Demonstration of a reduction in muscarinic receptor binding in early Alzheimer's disease using iodine-123 dexetimide single-photon emission tomography, Eur. J. Nucl. Med. 24 (1997) 602–608.

[11] J.M. Crook, B. Dean, G. Pavey, D. Copolov, The binding of [^{3}H]AF-DX384 is reduced in the caudate-putamen of subjects with schizophrenia, Life Sci. 64 (1999) 1761–1771.

[12] W.C. Eckelman, R.C. Reba, W. J. Rzeszotarski, R.E. Gibson, T. Hill, B.L. Holman, T. Budinger, J.J. Conklin, R. Eng, M.P. Grissom, External imaging of cerebral muscarinic acetylcholine receptors, Science 223 (1984) 291–294.

[13] C. Felder, F.P. Bymaster, J. Ward, N. DeLapp, Therapeutic opportunities for muscarinic receptors in the central nervous system, J. Med. Chem. 43 (2000) 4333–4353.

[14] D.D. Flynn, G. Ferrari-DiLeo, D.C. Mash, A.I. Levey, Differential regulation of molecular subtypes of muscarinic receptors in Alzheimer's Disease, J. Neurochem. 64 (1995) 1888–1891.

[15] D.D. Flynn, D.A. Weinstein, D.C. Mash, Loss of high-affinity antagonist binding to M_1 muscarinic receptors in Alzheimer's disease. Implication for the failure of cholinergic replacement therapies, Ann. Neurol. 29 (1991) 256.

[16] H.J. Grill, A. Heubner, K. Pollow, B. Manz, P.E. Schulze, H. Hofmeister, H. Laurent, R. Wiechert, W. Elger, (Z)-17β-Hydroxy-17 α-(2-[^{125}I]iodovinyl)-4-estren-3-one: A new specific gamma-emitting ligand for determination of progesterone receptor, J. Clin. Chem. Clin. Biochem. 25 (1987) 107–112.

[17] B.L. Holman, R.E. Gibson, T.C. Hill, W.C. Eckelman, M. Albert, R.C. Reba, Muscarinic acetylcholine receptors in Alzheimer's disease. *In vivo* imaging with iodine 123-labeled 3-quinuclidinyl 4-iodobenzilate and emission tomography, JAMA 254 (1985) 3063–3066.

[18] D.O. Kiesewetter, J.V. Silverton, W.C. Eckelman, Syntheses and biological properties of chiral fluoroalkyl quinuclidinyl benzilates, J. Med. Chem. 38 (1995) 1711–1719.

[19] A.I. Levey, Immunological localization of m1–m5 muscarinic acetylcholine receptors in peripheral tissues and brain, Life Sci. 52 (1993) 441–448.

[20] A.I. Levey, Muscarinic acetylcholine receptor expression in memory circuits: Implications for treatment of Alzheimer disease, Proc. Natl. Acad. Sci. USA 93 (1996) 13541–13546.

[21] A.I. Levey, C.A. Kitt, W.F. Simonds, D.L. Price, M.R. Brann, Identification and localization of muscarinic acetylcholinergic receptor proteins in brain with subtype-specific antibodies, J. Neurosci. 11 (1991) 3218–3226.

[22] D.W. McPherson, D.L. DeHaven-Hudkins, A.P. Callahan, F.F. Knapp Jr., Synthesis and biodistribution of iodine-125-labeled 1-azabicyclo[2.2.2]oct-3-yl α-hydroxy-α-(1-iodo-1-propen-3-yl)-α-phenylacetate. A new ligand for the potential imaging of muscarinic receptors by SPECT, J. Med. Chem. 36 (1993) 848–854.

[23] D.W. McPherson, M. Greenbaum, H. Luo, A.L. Beets, F.F. Knapp Jr., Evaluation of Z-R,R-IQNP for the potential imaging of the m2 mAChR rich regions of the brain and heart, Life Sci. 66 (2000) 885–896.

[24] D.W. McPherson, F.F. Knapp Jr., Structure elucidation via stereoselective synthesis of the acetate center of 1-azabicyclo[2.2.2]oct-3-yl α-hydroxy-α-(1-iodo-1-propen-3-yl)-α-phenylacetate (IQNP). A high affinity muscarinic imaging agent for SPECT, J. Org. Chem. 61 (1996) 8335–8337.

[25] D.W. McPherson, C.R. Lambert, F.F. Knapp Jr., In vivo metabolic studies of the trans-R,R isomer of radioiodinated IQNP: A new ligand with high affinity for the M_1 muscarinic-cholinergic receptor, Eur. J. Nucl. Med. 21 (1994) 1293–1297.

[26] D.W. McPherson, C.R. Lambert, K. Jahn, V. Sood, R.C. McRee, B. Zeeberg, R.C. Reba, F.F. Knapp Jr., Resolution, in vitro and in vivo evaluation of isomers of iodine-125-labeled 1-azabicyclo[2.2.2]oct-3-yl α-hydroxy-α-(1-iodo-1-propen-3-yl)-α-phenylacetate (IQNP). A high affinity ligand for the muscarinic receptor, J. Med. Chem. 38 (1995) 3908–3917.

[27] H.W. Muller-Gartner, H.S. Mayberg, R.S. Fisher, R.P. Lesser, A.A. Wilson, H.T. Ravert, R.F. Dannals, H.N. Wagner Jr., S. Uematsu, J.J. Frost, Decreased hippocampal muscarinic cholinergic receptor-binding measured by I-123 iododexetimide and single photon emission computed tomography in epilepsy, Ann. Neurol. 34 (1993) 235–238.

[28] H.W. Muller-Gartner, A.A. Wilson, R.F. Dannals, H.N. Wagner Jr., J.J. Frost, Imaging muscarinic cholinergic receptors in human brain in vivo with SPECT, [I-123]-4-iododexetimide and [I-123]-4-iodolevetimide, J. Cereb. Blood Flow Metab. 12 (1992) 562–570.

[29] K. Nobuhara, L. Farde, C. Halldin, P. Karlsson, C.G. Swahn, H. Olsson, K.A. Bergstrom, S.A. Larsson, P.O. Schnell, D.W. McPherson, A. Savonen, J. Hiltunen, G. Sedvall, SPECT imaging of central muscarinic acetylcholine receptors with iodine-123 labelled E-IQNP and Z-IQNP, Eur. J. Nucl. Med. 28 (2001) 13–24.

[30] K. Nobuhara, C. Halldin, H. Hall, P. Karlsson, L. Farde, J. Hiltunen, D.W. McPherson, A. Savonen, K.A. Bergstrom, P. Stefan, C.G. Swahn, S.A. Larsson, P.O. Schnell, G. Sedvall, Z-IQNP: A potential radioligand for SPECT imaging of muscarinic acetylcholine receptors in Alzheimer's disease, Psychopharmacology (Berl) 149 (2000) 45–55.

[31] A. Nordberg, I. Alaguzoff, B. Winblad, Nicotinic and muscarinic subtypes in the human brain: Changes with aging and dementia, J. Neurosci. Research 31 (1992) 103–111.

[32] M.R. Rayeq, S.F. Boulay, V.K. Sood, D.W. McPherson, F.F. Knapp Jr., B.R. Zeeberg, R.C. Reba, In vivo autoradiographic evaluation of isomers of I-125-labeled 1-azabicyclo[222]oct-3-yl α-hydroxy-α-(1-iodo-1-propen-3-yl)-α-phenylacetate (IQNP). Direct evidence for enhanced *in vivo* M, 2 muscarinic subtype selectivity for Z-(-)(-)-[^{125}I]-IQNP, Receptors and Signal Transduction 6 (1996) 13–34.

[33] K.J. Reinikainen, P.J. Riekkinen, T. Halonen, M. Laakso, Decreased muscarinic receptor binding in cerebral cortex and hippocampus in Alzheimer's disease, Life Sci. 41 (1987) 453–461.

[34] W.J. Rzeszotarski, D.W. McPherson, J.W. Ferkany, W.J. Kinnier, L. Noroha-Blob, A. Kirken-Rzeszotarski, Affinity and selectivity of the optical isomers of 3-quinuclidinyl benzilate and related muscarinic antagonists, J. Med. Chem. 31 (1988) 1463–1466.

[35] H. Shinotoh, M. Asahina, O. Inoue, T. Suhara, K. Hirayama, Y. Tateno, Effects of trihexyphenidyl and L-dopa on brain muscarinic cholinergic receptor binding measured by positron emission tomography, J. Neural. Transm. [P-D Sect] 7 (1994) 35–46.

[36] M.B. Skaddan, M.R. Kilbourn, S.E. Snyder, P.S. Sherman, T.J. Desmond, K.A. Frey, Synthesis, ^{18}F-labeling, and biological evaluation of piperidyl and pyrrolidyl benzilates as in vivo ligands for muscarinic acetylcholine receptors, J. Med. Chem. 43 (2000) 4552–4562.

[37] H.A. Stabb, Synthesis using heterocyclic amides (Azolides), Angew Chem. Intern. Edit. 1 (1962) 351–367.

[38] Y. Sudo, T. Suhara, Y. Honda, T. Nakajima, Y. Okubo, K. Suzuki, Y. Nakashima, K. Yoshikawa, T. Okauchi, Y. Sasaki, M. Matsushita, Muscarinic cholinergic receptors in human narcolepsy: A PET study, Neurology 51 (1998) 1297–1302.

[39] T. Suhara, O. Inoue, K. Kobayashi, T. Satoh, Y. Tateno, An acute effect of triazolam on muscarinic cholinergic receptor binding in the human brain measured by positron emission tomography, Psychopharmacology (Berl) 113 (1994) 311–317.

[40] T. Suhara, O. Inoue, K. Kobayashi, K. Suzuki, Y. Tateno, Age-related changes in human muscarinic acetylcholine receptors measured by positron emission tomography, Neurosci. Lett. 149 (1993) 225–228.

[41] T. Sunderland, G. Esposito, S.E. Molchan, R. Coppola, D.W. Jones, J. Gorey, J.T. Little, M. Bahro, D.R. Weinberger, Differential cholinergic regulation in Alzheimer's patients compared to controls following chronic blockade with scopolamine: A SPECT study, Psychopharmacology (Berl) 121 (1995) 231–241.

[42] Y. Swada, S. Hiraga, B. Francis, C. Patlak, K. Pettigrew, K. Ito, E. Owens, R. Gibson, R. Reba, W. Eckelman, S. Larson, R. Blasberg, Kinetics analysis of 3-quinuclidinyl 4-[^{125}I]iodobenzilate transport and specific binding to muscarinic acetylcholine receptor in rat brain *in vivo*: implications for human studies, J. Cereb. Blood Flow Metab. 10 (1990) 781–807.

[43] S.M. Terjani-Butt, G.R. Luthin, B.B. Wolfe, D.J. Brunswick, N-Substituted derivatives of 4-piperidinyl benzilate: Affinities for brain muscarinic acetylcholine receptors, Life Sci. 47 (1990) 841–848.

[44] M. Weckesser, A. Hufnagel, K. Ziemons, M. Griessmeier, F. Sonnenberg, T. Hacklander, K.J. Langen, M. Holschbach, C.E. Elger, H. W. Muller-Gartner, Effect of partial volume correction on muscarinic cholinergic receptor imaging with single-photon emission tomography in patients with temporal lobe epilepsy, Eur. J. Nucl. Med. 24 (1997) 1156–1161.

[45] D.R. Weinburger, R. Gibson, R. Coppola, D.W. Jones, S. Molchan, T. Sunderland, K.F. Berman, R.C. Reba, The distribution of cerebral muscarinic acetylcholine receptors *in vivo* in patients with dementia. A controlled study with ^{123}IQNB and single photon emission computed tomography, Arch. Neurol. 48 (1991) 169–176.

[46] D.R. Weinburger, D. Jones, R.C. Reba, U. Mann, R. Coppola, R. Gibson, J. Gorey, S.A. Braun, T.N. Chase, A comparison of FDG PET and IQNB SPECT in normal subjects and in patients with dementias, J. Neuropsychiatry Clinical Neursci. 4 (1992) 239–248.

[47] D.R. Weinburger, D. Jones, T. Sunderland, K.S. Lee, R. Sexton, J. Gorey, R.C. Reba, In vivo imaging of cerebral muscarinic receptors with I-123 QNB and SPECT: Studies in normal subjects and patients with dementias, Clin. Neuropharmacol. 15 (1992) 194A–195A.

[48] J. Wyper, D. Brown, J. Patterson, J. Owens, R. Hunter, E. Teasdale, J. McCulloch, Deficits in iodine-labelled 3-quinuclidinyl benzilate binding in relation to cerebral blood flow in patients with Alzheimer's disease, Eur. J. Nucl. Med. 20 (1993) 379–386.

[49] T. Yoshida, Y. Kuwabara, Y. Ichiya, M. Sasaki, T. Fukumura, A. Ichimiya, M. Takita, K. Ogomori, K. Masuda, Cerebral muscarinic acetylcholinergic receptor measurement in Alzheimer's disease patients on ^{11}C-N-methyl-4-piperidinyl benzilate. Comparison with cerebral blood flow and cerebral glucose metabolism, Ann. Nucl. Med. 12 (1998) 35–42.

[50] K. Zilles, M. Qu, A. Schleicher, M. Schroeter, M. Kraemer, O.W. Witte, Plasticity and neurotransmitter receptor changes in Alzheimer's disease and experimental cortical infarcts, Arzneim.-Forsch/Drug Res. 45 Nr. 3a (1995) 361–366.

[51] J.K. Zubieta, R.A. Koeppe, G.K. Mulholland, D.E. Kuhl, K.A. Frey, Quantification of muscarinic cholinergic receptors with [^{11}C]NMPB and positron emission tomography: Method development and differentiation of tracer delivery from receptor binding, J. Cereb. Blood Flow Metab. 18 (1998) 619–631.